2021

Material Selection and Sizing of a Thermoelectric Generator (TEG) for Power Generation in a Self-Powered Heating System

Tim J. LaClair
Oak Ridge National Laboratory, laclairtj@ornl.gov

Kyle R. Gluesenkamp
Oak Ridge National Laboratory

Hsin Wang
Oak Ridge National Laboratory

Ahmad Abuheiba
Oak Ridge National Laboratory

Praveen Cheekatamarla
Oak Ridge National Laboratory

See next page for additional authors

Material Selection and Sizing of a Thermoelectric Generator (TEG) for Power Generation in a Self-Powered Heating System

Tim J. LACLAIR[1]*, Kyle R. GLUESENKAMP[1], Ahmad ABU-HEIBA[1], Praveen CHEEKATAMARLA[1], Hsin WANG[1], Sandeep ALAVANDI[2], Hamid ABBASI[2], David CYGAN[2], Alexander KIRK[2], and Uttam GHOSHAL[3]

[1]Oak Ridge National Laboratory
Oak Ridge, Tennessee, USA
Contact: laclairtj@ornl.gov | 865-341-1305

[2]Gas Technology Institute
Des Plaines, Illinois, USA
Contact: salavandi@gti.energy | 847-768-0571

[3]Sheetak Inc.,
Austin, Texas, USA
Contact: ghoshal@sheetak.com | 512-382-0744

* Corresponding Author

ABSTRACT

By employing the high temperature heat source to directly generate the electricity needed to power auxiliary systems in a natural gas furnace, boiler or hot water heater, a "self-powered" heating system can provide several benefits. Compared with a traditional furnace, boiler or hot water heater, when overall fuel utilization is kept constant, the self-powered system will have a higher primary energy efficiency, lower operating costs, and dramatically improved building safety and resilience during electric grid outages. Furthermore, a self-powered heating system only has a single utility connection – natural gas, without an electric connection – thus simplifying installation. A thermoelectric generator can be used for direct energy conversion of thermal energy to electricity with no moving parts, which offers a very simple means to provide power for the self-powered heating system, and the operation is without noise or vibration and can thus provide a very long system life. This paper provides an analysis focused on materials selection and the thermal power requirements for a thermoelectric generator (TEG) for use in a self-powered heating system. The dimensionless figure of merit for thermoelectric materials, zT, is used to estimate the optimal efficiency that can be achieved with a TEG to produce the electric power required in such an application. Comparisons of the predicted efficiency, the required heat transfer rate to the TEG and the heat transfer area needed for sustained operation under thermal conditions relevant to the self-powered heating application are made for several potential thermoelectric materials. This analysis was used to develop system requirements for a self-powered hot water heater using a TEG for electric power generation.

1. INTRODUCTION

Conventional natural gas heating systems employed in buildings (furnaces, boilers and water heaters) require an electrical supply to power auxiliary equipment such as fans, ignitor and electronic controllers, requiring a second utility connection to the heating system even though electricity is not employed for the heating. These heating devices cannot function during power outages, which can eliminate the ability to provide heat when it is most needed, for

example following severe storms when temperature extremes may be experienced for extended periods. Therefore, a self-powered heating system—one that generates its own electrical power as opposed to being connected to the electric grid—can improve building safety and resilience during electric grid outages. Additionally, a self-powered device simplifies installation since only a single utility connection is required, and there are potential benefits in primary energy usage when the power is generated locally (Gluesenkamp, 2019). Self-powered heating systems, including furnaces, boilers and hot water heaters, have been investigated in previous studies, and the literature shows examples of systems utilizing several possible power cycles for the electrical generation. A review of power conversion options for self-powered furnaces is provided in Abu-Heiba *et al*. (2021). Some specific applications are described in the following. Qiu and Hayden (2008) reported development of a self-powered residential hydronic heating system for which a PbSnTe thermoelectric generator (TEG) was used as the electricity generation device. The system generated 553.9 W of electric power at a hot surface temperature of 637°C and a cold surface temperature of 85°C. Butcher *et al*. (2011) built an oil-fired self-powered boiler that employed a thermophotovoltaic (TPV) module for the power generation, with a targeted electrical output of 100 W. Various emitter material systems and GaSb TPV cell configurations were evaluated for the impact on the heat transfer efficiency to the emitter. Qiu and Hayden (2014) integrated a GaSb TPV generator into a residential combi boiler. A maximum power of 246.4 W at an emitter temperature of 1265°C was generated with a fuel input of 12.3 kW. Alptekin *et al*. (2017) developed a self-powered condensing combi boiler based on a TEG for electrical generation, and the system was evaluated experimentally at several different firing and water flow rates.

This paper focuses on TEG materials for electric power generation in self-powered heating systems. A methodology for TEG material evaluation is used to characterize the performance of several TEG materials for use in natural gas applications, and associated thermal power requirements are evaluated.

2. MATERIAL PROPERTY CONSIDERATIONS FOR THERMOELECTRIC DEVICES

2.1 Thermoelectric Material Figure of Merit

The dimensionless thermoelectric (TE) figure of merit, zT, for a single p-type or n-type material is given by Equation (1),

$$zT = \left(\frac{S^2}{\rho k}\right)T, \tag{1}$$

where S is the Seebeck coefficient, ρ is the electrical resistivity, k is the thermal conductivity, and T is the absolute temperature (Rowe, 2006). It is noted that a TEG requires a combination of both p- and n-type materials, while the figure of merit zT is defined for individual materials. Nonetheless, this property provides a convenient and useful metric of the TE performance of individual materials for use in TE devices and is frequently reported as a function of temperature in the literature. In this report, zT data was obtained for 16 materials (Bjork, 2015) covering the feasible temperature range of each material. The data was digitized so detailed numerical analysis could be conducted for material selection and sizing for the TEG design. Figure 1 shows the zT data for these materials.

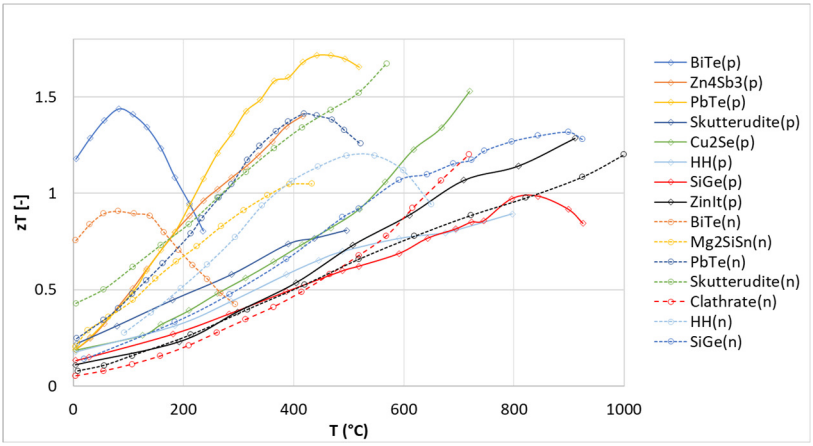

Figure 1: Dimensionless material-specific figure of merit, zT, for p- and n-type thermoelectric materials. [Data from Bjork (2015)]

A TEG consists of p- and n-type TE materials that are connected electrically in series and thermally in parallel, as shown in Figure 2.

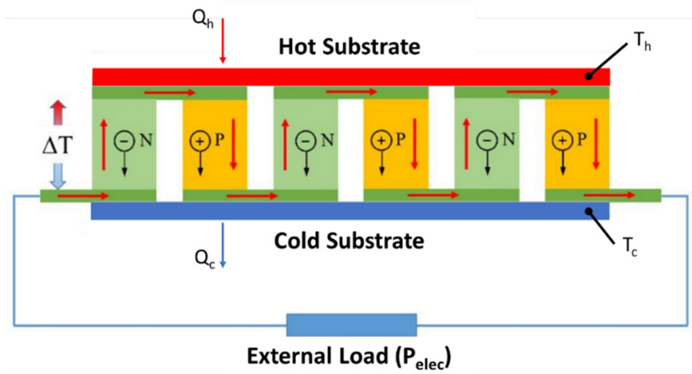

Figure 2: TEG operation: heat is transferred from an external source at the rate Q_h, and removed at the rate Q_c. Electrical power, P_{elec}, is generated by the TEG and provided to an external load.

2.2 TEG Device Figure of Merit

The device figure of merit, Z, for a TEG is given by

$$Z = \frac{(S \quad S)^2}{[(\rho k)^{1/2} + (\rho k)^{1/2}]^2}, \tag{2}$$

where the subscripts correspond to the p- and n-type materials used for each couple in the TEG. Under some conditions, the value of Z can be reasonably approximated as the mean of the material figures of merit, z_p and z_n. The TEG efficiency, η, is defined as the electrical output divided by the high temperature thermal input ($\eta = P_{elec}/Q_h$). Once a value of Z is determined, the TEG maximum efficiency, η, can be calculated according to Equation (3):

$$\eta = \Delta T/T_h \left(\sqrt{(1+ZT)} - 1\right) / \left(\sqrt{(1+ZT)} + \frac{T_c}{T_h}\right), \tag{3}$$

where T_c and T_h are the cold- and hot-side substrate temperatures of the TEG, and ΔT is the temperature difference T_h-T_c across the TEG (Bjork, 2015). For the analysis in this work, the value of ZT was evaluated at the average operating temperature of the TEG, $T_{avg}=(T_c+T_h)/2$, and Z was approximated as the mean of z_n and z_p at T_{avg}, as described previously. For comparison purposes, the ZT determined from average zT values are shown in Figure 3 as a function of average TEG temperature for combinations of p- and n-type TE materials based on the same un-doped material.

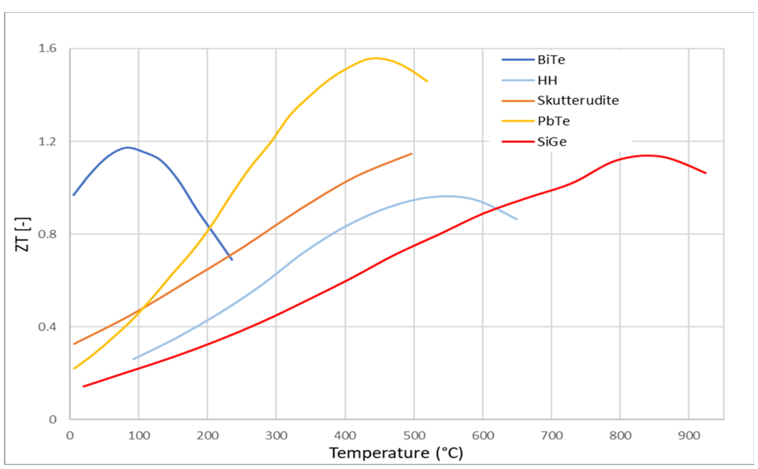

Figure 3: Dimensionless device figure of merit, ZT, as a function of average temperature for TEGs based on p- and n-type materials derived from BiTe, Half-Heusler, Skutterudite, PbTe and SiGe.

3. TEG PEAK EFFICIENCY, REQUIRED HEAT TRANSFER AND DEVICE AREA FOR DIFFERENT MATERIALS

Equation (3) for the TEG efficiency is used to determine and compare device efficiencies, which are subsequently used to calculate thermal power requirements and required TEG sizing based on different materials. These results are presented individually for the set of materials shown in Figure 3 at different operating conditions/boundary conditions relevant to the hot water heater operation. Then, plots are presented for each material at individual operating conditions to allow direct comparisons of the performance expected based on material selection.

3.1 Bismuth Telluride, BiTe

The calculated efficiency as a function of T_h for a TEG composed of n- and p-type bismuth telluride (BiTe) is shown in Figure 4 for three levels of T_c (50, 100 and 200°C), which are used throughout the analysis.

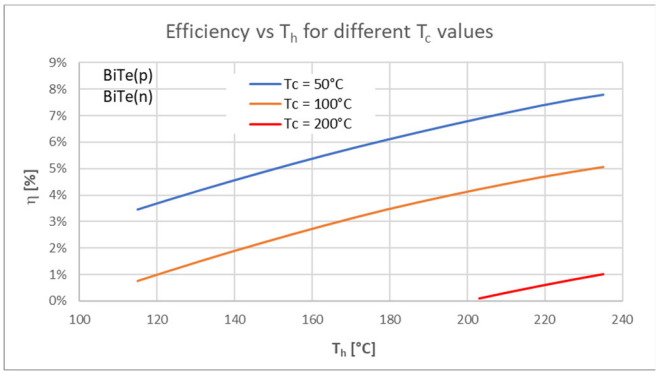

Figure 4: Maximum efficiency as a function of T_h and T_c for a TEG based on BiTe(p) and BiTe(n).

Since the TEG's conversion efficiency is the ratio of the electric power output to the thermal power input to the device, the rate of heat transfer, Q_h, that must be provided to the TEG from the heat source can be calculated from the efficiency and the required electrical power output, P_{elec}, as shown in Equation (4).

$$Q_h = \frac{P_{elec}}{\eta} \tag{4}$$

Figure 5 shows the thermal power required for the BiTe(p)-BiTe(n) TEG, per 100 W_{elec} of required electric power.

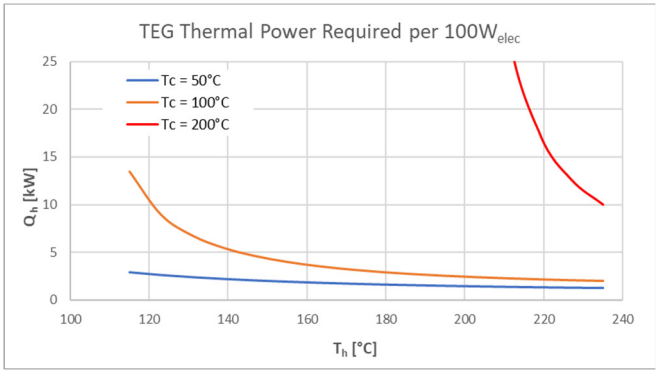

Figure 5: Required heat transfer rate to the TEG per 100 W electric power as a function of T_h and T_c for a TEG based on BiTe (p) and BiTe (n).

The heat transfer to the TEG hot side comes from an external heat source (e.g. a combustion gas stream), and heat must also be removed from the TEG cold side. For each side (hot and cold), there is an overall heat transfer coefficient that couples the external source and sink temperatures ($T_{h,\infty}$ and $T_{c,\infty}$) to the hot and cold substrate temperatures T_h and T_c, respectively. The heat transfer area, A, of each surface and the overall heat transfer coefficient, U, determine the heat transfer rate to/from the TEG. It should be noted that an array of TEG's may be required to achieve the desired power output for practical applications. Furthermore, the power output of the materials could be reduced due to

parasitic electrical losses or Joule heating, and heat transfer losses should be considered when estimating the overall heat transfer coefficient to the TEG since they could potentially lower the electrical power output.

For the hot side, the heat transfer rate is given by

$$Q_h = U_h A_h (T_{h,\infty} - T_h) = U_h A_h \Delta T_h \quad (5)$$

and a similar relation governs the heat removal from the cold side:

$$Q_c = U_c A_c (T_c - T_{c,\infty}) = U_c A_c \Delta T_c \quad (6)$$

By inspection of Equation (6), it is clear that T_c will decrease with increasing $U_c A_c$ and will increase with decreasing $U_c A_c$. Therefore, without precisely calculating all parameters on the cold side, we can parameterize our analysis very simply by considering a few assumed T_c values that would be expected for $T_{c,\infty}$=20°C. We considered three cases for T_c: 50°C, 100°C and 200°C for high, medium and low $U_c A_c$ cases, respectively.

Returning to our analysis of the hot side heat transfer and sizing, Equation (4) provides Q_h as a function of T_h for the three considered levels of T_c (see Figure 5). Then $U_h A_h$ is uniquely determined when $T_{h,\infty}$ is specified, according to Equation (5). Depending on where the TEG is placed in the hot water heater, we can assume a value for $T_{h,\infty}$ ranging up to about 1400°C (if using the flame or combustion gases as the source). The overall heat transfer coefficient U_h will depend on how the TEG is thermally coupled to the burner/HX, but it can be reasonably approximated. For a typical forced convection heat transfer coefficient to air, we can expect a h value on the order of 100 W/m^2-K, but considering the additional resistances through a heat exchanger and to the TEG from the combustion gases will result in a lower overall heat transfer coefficient. We assume a value of U_h=50 W/m^2-K for the remainder of this analysis.

Our conclusion resulting from this reasoning is that the heat transfer area A_h is also determined as a function of T_h for each of the $U_c A_c$ levels considered (high, medium, low). The resulting A_h is the minimum surface area required at the hot side of the TEG to provide the heat transfer rate necessary for the TEG to sustain the specified electric power output P_{elec}. The proper equation is obtained by combining Equations (4) and (5). The final result is

$$A_h = \frac{P_{elec}}{U_h (T_{h,\infty} - T_h (\eta(T_h; T_c))} \quad (7)$$

Considering the effect of the hot-side heat transfer coefficient on the required heat transfer area, from Equation (7) it can be noted that A_h is inversely proportional to U_h, independent of the other parameters used in the analysis. This indicates that the required heat transfer area will decrease by the same proportion as any increase in the overall heat transfer coefficient, emphasizing the importance of maximizing the coefficient between the heat source and the TEG.

Figure 6 shows the hot side area required per 100 W of electric power generation for the BiTe-based TEG with an assumed $T_{h,\infty}$ = 1400°C. Note that this source temperature significantly exceeds the temperature limit for the TEG, so it is assumed that the heat exchanger will maintain the hot substrate at a feasible temperature and that sufficient cooling at the cold side is always available to maintain the hot-side temperature of the TEG below its upper limit of operation.

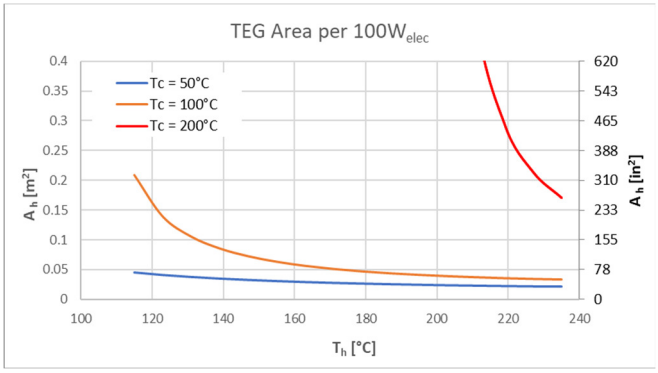

Figure 6: Required hot side heat transfer area, per 100 W electric power, as a function of T_h and T_c for a TEG based on BiTe (p) and BiTe (n).

3.2 Lead Telluride, PbTe

Using the equations for the efficiency, thermal power requirement and required heat transfer area as a function of the TEG hot- and cold-side temperatures, we compare results for the different TE materials. The same assumptions for U_h and $T_{h,\infty}$ are used in all cases to provide a "clean" comparison. Figure 7 shows the result of calculations for PbTe(p) and PbTe(n) materials. The ability to operate at higher temperatures and the higher zT values for this material result in considerably higher maximum efficiency than the BiTe material considered previously. Although for the same T_h operating range, the BiTe actually had higher efficiency, the PbTe can function at temperatures over 500°C (vs. only 235°C for BiTe), which enables a larger temperature difference and a greater maximum efficiency. For use in the hot water heater application, using the natural gas flame with temperatures of approximately 1400°C as the TEG's heat source, it makes sense to take advantage of the material enabling the higher temperature operation. We see at the highest hot side temperatures, the required thermal power and area are quite insensitive to the cold side temperature.

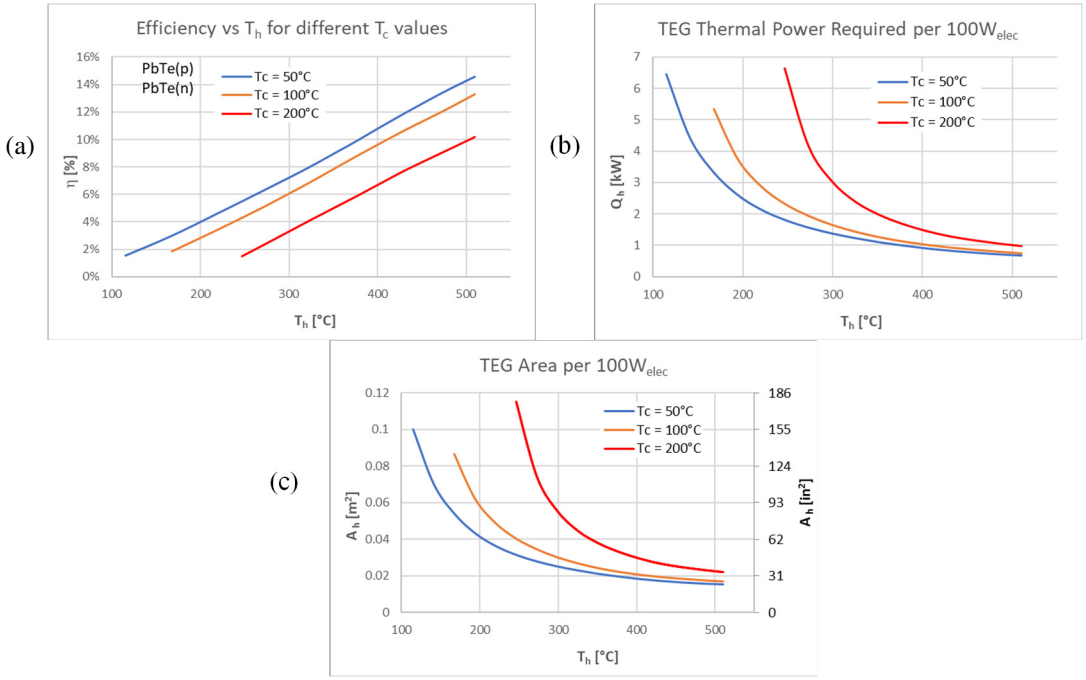

Figure 7: (a) TEG Efficiency, (b) Thermal power requirement per 100W electric power, and (c) required TEG heat transfer area for a TEG based on PbTe (p) and PbTe (n).

3.3 Half-Heusler, HH

Figure 8 shows results for a TEG based on Half-Heusler (HH) p- and n-type materials. The peak TEG efficiency is less for this material than for the lower temperature PbTe materials since the ZT value is considerably lower for the HH.

3.4 Skutterudite

Figure 9 shows the results for a TEG based on Skutterudite p- and n-type materials. The results appear fairly similar to those for the PbTe p- and n-type TEG, except that the maximum temperature is a little lower for the Skutterudite and its maximum efficiency at peak operating temperature is reduced considerably due to the lower ZT of Skutterudite material at temperatures approaching the limits of its operating range.

3.5 Silicon Germanium, SiGe

Figure 10 shows the results for the TEG based on SiGe(p) and SiGe(n) materials. The area requirement begins to increase very slightly for T_h>800°C. Although the device efficiency increases up to the maximum temperature, due to the decrease in the driving temperature difference ΔT_h as the hot side temperature is increased, the area requirement increases with rising T_h, so there is no benefit in terms of sizing obtained from the increased efficiency. For this material, if the source temperature could be increased to $T_{h,\infty}$ = 1800°C, the minimum heat transfer area required decreases to approximately 0.017 m^2 (26 in^2) per 100W electric power produced, but at the flame temperatures typical in a hot water heater, the performance does not reach the same level as for any of the previously considered materials.

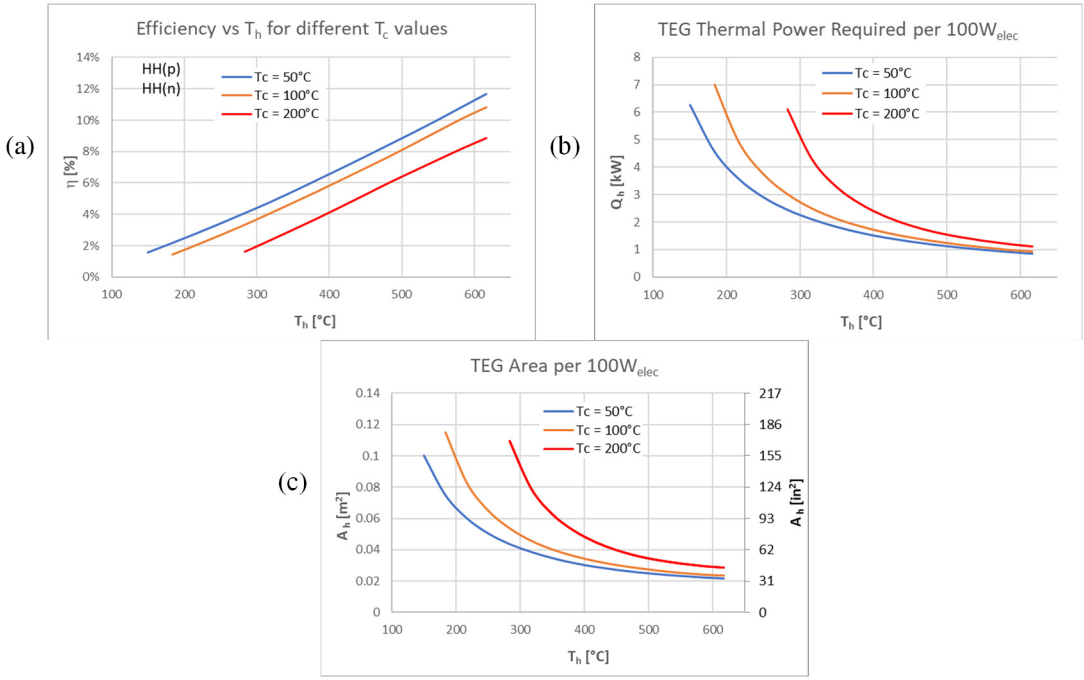

Figure 8: (a) TEG Efficiency, (b) Thermal power requirement per 100W electric power, and (c) required TEG heat transfer area for a TEG based on HH (p) and HH (n).

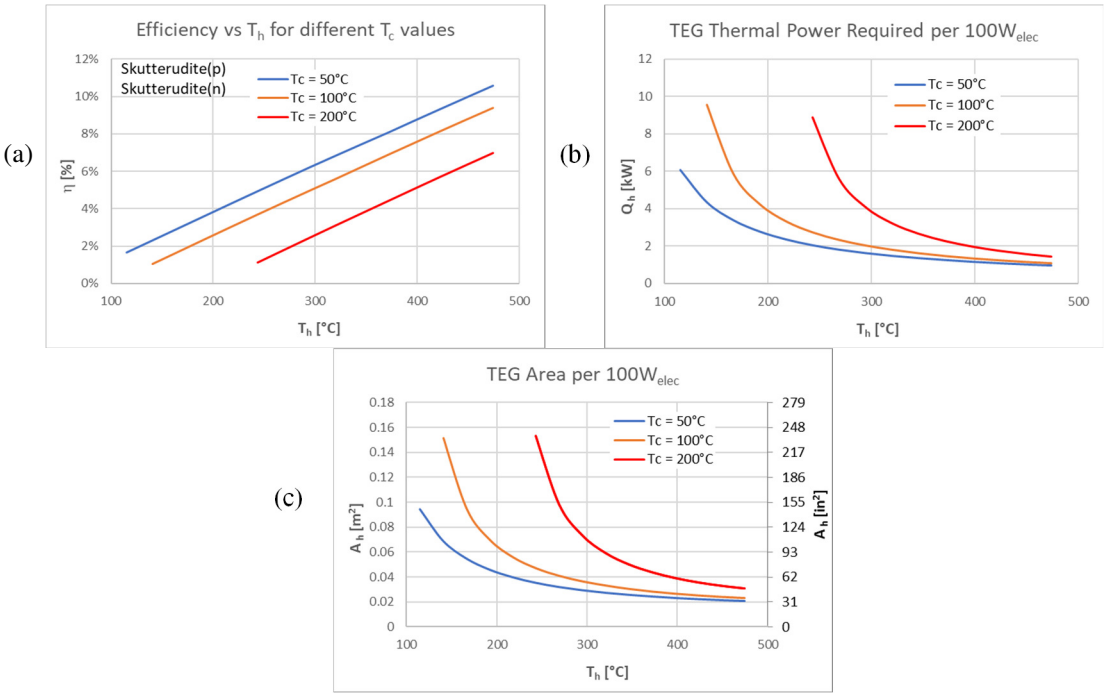

Figure 9: (a) TEG Efficiency, (b) Thermal power requirement per 100 W electric power, and (c) required TEG heat transfer area for a TEG based on Skutterudite (p) and Skutterudite (n).

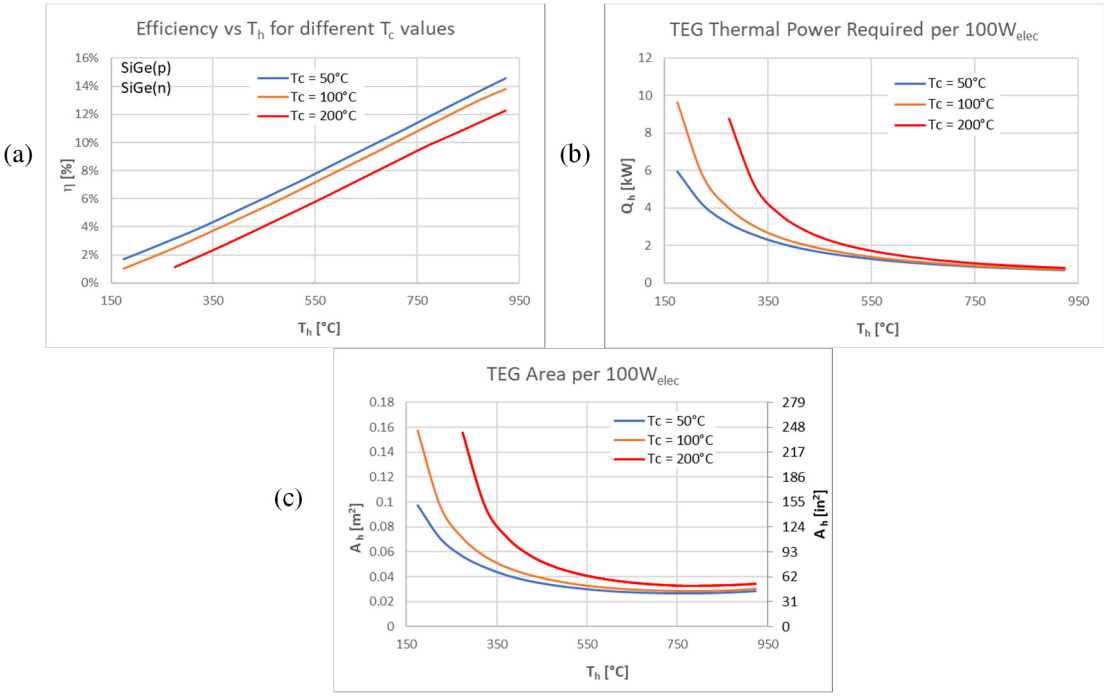

Figure 10: (a) TEG Efficiency, (b) Thermal power requirement per 100 W electric power, and (c) required TEG heat transfer area for a TEG based on SiGe(p) and SiGe(n).

4. PERFORMANCE COMPARISON PLOTS BETWEEN TE MATERIALS

To provide a direct comparison of results for different material selections, the Q_h and A_h curves are shown in Figure 11 for T_c=50°C and Figure 12 for T_c=200°C, for the five primary material combinations considered above (p- and n-type materials derived from the same undoped materials). The results in Figure 12 do not include BiTe, since for this material the upper operating temperature is only about 235°C, and the high T_c value would allow only a very narrow band of operation.

The results from this analysis show that TEG material with the lowest required heat transfer area depends on the cold side substrate temperature, T_c. For T_c=50°C (Figure 11), the lowest heat transfer area is achieved with PbTe, although BiTe can provide the same power with a very similar area while operating at a much lower hot-side temperature. SiGe can provide the highest power output for a given temperature difference and it can handle much higher temperatures, although the area requirement is higher due to a lower efficiency. For T_c=200°C (Figure 12), the smallest area can be achieved with a TEG utilizing PbTe. Further improvements in efficiency can be achieved and the required heat transfer area can be reduced if higher source temperature can be used, and also if the thermal coupling of the TEG to the heat source is increased. Improved coupling to the cold sink improves the performance of the TEG, but the performance is much more sensitive to $U_h A_h$ than to $U_c A_c$. In the results for PbTe presented in Figure 7, at T_h=500°C, increasing the value of U_h would result in a *proportional* increase in the heat transfer Q_h to the TEG and a corresponding decrease in required heat transfer area. On the other hand, doubling U_c (i.e. reducing T_c) produces only about a 5% reduction in area at the most effective operating condition.

5. CONCLUSIONS

Parametric analyses were conducted to evaluate the impacts of different operating conditions, including the hot- and cold-side temperatures of the TEG substrate, and the temperature of the heat source. These parameters are convenient for the TEG analysis and can be determined from the specific design configuration of the TEG in the self-powered hot water heater. Based on expected operating temperatures for our application, the model predicts that the p- and n-type PbTe material can provide the required power using the smallest size TEG device. Although SiGe allows higher operating temperatures and the greatest power output for a given temperature difference, its efficiency remains lower until much higher substrate temperatures are reached, and a larger heat transfer area is required. Bismuth telluride,

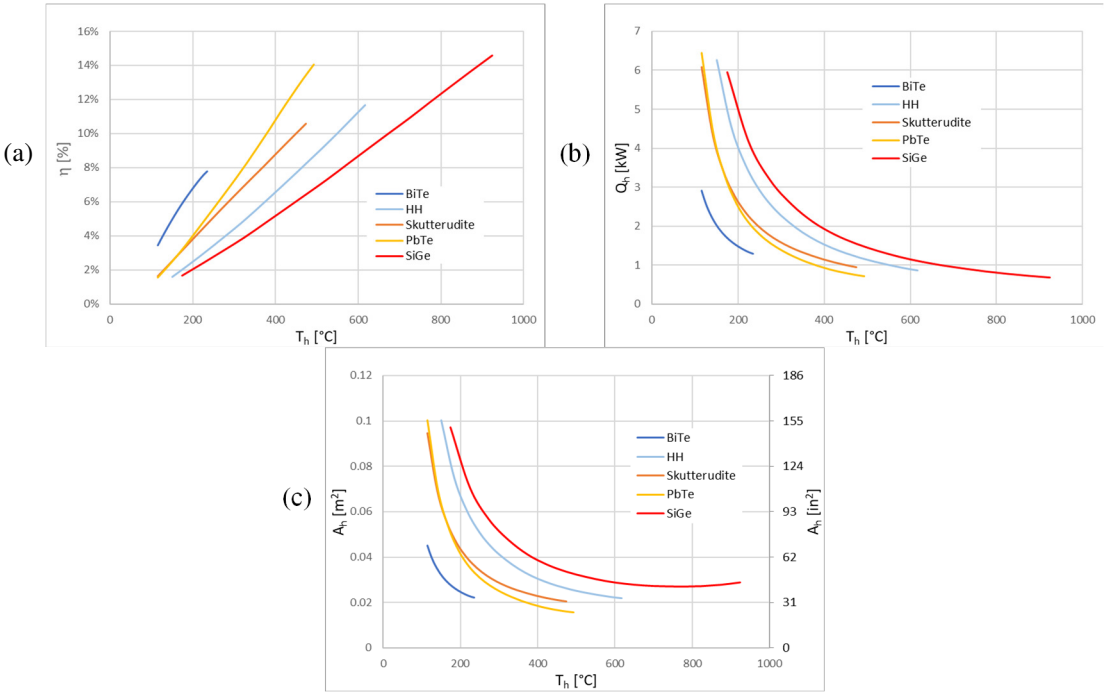

Figure 11: (a) Efficiency, (b) thermal power requirement per 100 W electric power, and (c) required TEG heat transfer area for the primary materials considered above. Results correspond to the lowest heat transfer performance on the cold side, i.e. T_c=50°C.

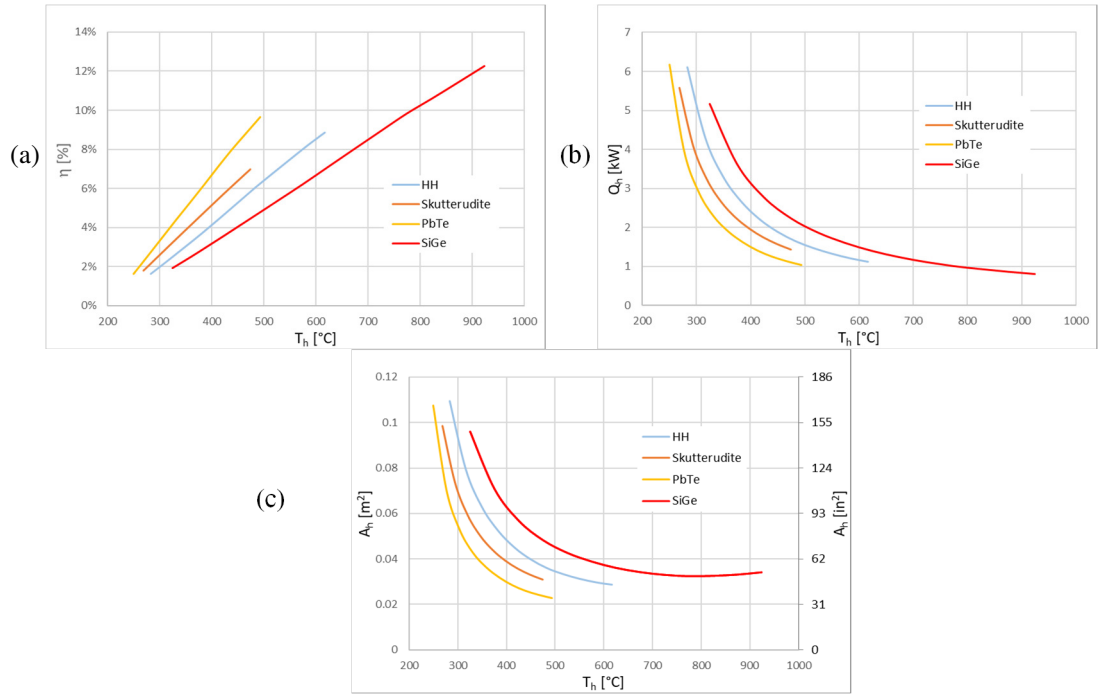

Figure 12: (a) Efficiency, (b) thermal power requirement per 100 W electric, and (c) required TEG heat transfer area for the primary materials. Results are for the lowest heat transfer performance on the cold side, i.e. T_c=200°C.

which is readily available on the commercial market, is limited to temperatures below 250°C, which limits the efficiency that can be achieved in the hot water heater application, unless the cold substrate temperature is kept quite cool (for example, 50°C). Skutterudite and Half-Heusler materials operate in a similar temperature range as the lead telluride, but the efficiency is somewhat reduced and a larger TEG would be required to generate the required power. We note that, other than bismuth telluride, there are few commercially available high temperature modules on the market, and development of customized TEGs would likely be required for other materials, although there have been recent product additions. Furthermore, in practical systems the efficiency will be lower than the ideal conditions due to thermal and electrical interface losses and long-term degradation.

NOMENCLATURE

A	area
k	thermal conductivity
P	power
Q	heat transfer rate
S	Seebeck coefficient
T	absolute temperature
ΔT	temperature difference across a TEG
U	overall heat transfer coefficient
z	material figure of merit for a TEG
Z	device figure of merit for a TEG
η	efficiency
ρ	electrical resistivity

Subscript

avg	average
c	cold side
elec	electrical
h	hot side
n	n-type material used for a couple in a TEG
p	p-type material used for a couple in a TEG
∞	source or sink

REFERENCES

Abu-Heiba, A., Gluesenkamp, K. R., LaClair, T. J., Cheekatamarla, P., Munk, J., Thomas, J., Boudreaux, P. (2021). Analysis of power conversion technology options for a self-powered furnace. *Appl. Therm. Eng.* (Accepted for publication).

Alptekin, M., Calisir, T., & Baskaya, S. (2017). Design and experimental investigation of a thermoelectric self-powered heating system. *Energy Conversion and Management, 146*, 244-252.

Bjork, R. (2015). Universal influence of contact resistance on the efficiency of a thermoelectric generator. *J. Electron. Mater., 44*(8), 2869-2876.

Butcher, T. A., Hammonds, J. S., Horne, E., Kamath, B., Carpenter, J., & Woods, D. R. (2011). Heat transfer and thermophotovoltaic power generation in oil-fired heating systems. *Applied Energy, 88*(5), 1543-1548.

Gluesenkamp, Kyle R. (2019). Drop-in, retrofit furnace with maximum efficiency – self powered system." DOE Building Technologies Office 7th Annual Peer Review, April 15–10, 2019, Crystal City, Virginia. Available at https://www.energy.gov/sites/prod/files/2019/05/f62/bto-peer%E2%80%932019-ornl-drop-in-retrofit-furnace-max-eff.pdf

Qiu, K. & Hayden, A. C. S. (2008). Development of a thermoelectric self-powered residential heating system. *Journal of Power Sources*, 180(2), 884-889.

Qiu, K. & Hayden, A. C. S. (2014). Implementation of a TPV integrated boiler for micro-CHP in residential buildings. *Applied Energy*, *134*, 143-149.

Rowe, D. M. (2006). *Thermoelectrics Handbook—Macro to Nano*. Boca Raton, FL: Taylor and Francis Group.